Free Radical Biology and Medicine 71 (2014) 146–156

Contents lists available at ScienceDirect

Free Radical Biology and Medicine

journal homepage: www.elsevier.com/locate/freeradbiomed

Original Contribution

Acute hypoxia produces a superoxide burst in cells

Pablo Hernansanz-Agustín [a,b], Alicia Izquierdo-Álvarez [a], Francisco J. Sánchez-Gómez [c,d,1], Elena Ramos [a], Tamara Villa-Piña [a], Santiago Lamas [c,d], Anna Bogdanova [e], Antonio Martínez-Ruiz [a,*]

[a] Servicio de Inmunología, Hospital Universitario de La Princesa, Instituto de Investigación Sanitaria Princesa, E-28006 Madrid, Spain
[b] Departamento de Bioquímica, Facultad de Medicina, Universidad Autónoma de Madrid and Instituto de Investigaciones Biomédicas Alberto Sols, E-28029 Madrid, Spain
[c] Laboratorio Mixto, Consejo Superior de Investigaciones Científicas/Fundación Renal "Iñigo Alvarez de Toledo," E-28049 Madrid, Spain
[d] Departamento de Biología Celular e Inmunología, Centro de Biología Molecular "Severo Ochoa," Consejo Superior de Investigaciones Científicas–Universidad Autónoma de Madrid, E-28049 Madrid, Spain
[e] Institute of Veterinary Physiology, Vetsuisse Faculty, and Zurich Center for Integrative Human Physiology, University of Zurich, CH-8057 Zurich, Switzerland

ARTICLE INFO

Article history:
Received 28 January 2014
Received in revised form
7 March 2014
Accepted 8 March 2014
Available online 15 March 2014

Keywords:
Hypoxia
Ischemia
Cell signaling
Superoxide
Reactive oxygen species
Oxidative phosphorylation
Free radicals

ABSTRACT

Oxygen is a key molecule for cell metabolism. Eukaryotic cells sense the reduction in oxygen availability (hypoxia) and trigger a series of cellular and systemic responses to adapt to hypoxia, including the optimization of oxygen consumption. Many of these responses are mediated by a genetic program induced by the hypoxia-inducible transcription factors (HIFs), regulated by a family of prolyl hydroxylases (PHD or EGLN) that use oxygen as a substrate producing HIF hydroxylation. In parallel to these oxygen sensors modulating gene expression within hours, acute modulation of protein function in response to hypoxia is known to occur within minutes. Free radicals acting as second messengers, and oxidative posttranslational modifications, have been implied in both groups of responses. Localization and speciation of the paradoxical increase in reactive oxygen species production in hypoxia remain debatable. We have observed that several cell types respond to acute hypoxia with a transient increase in superoxide production for about 10 min, probably originating in the mitochondria. This may explain in part the apparently divergent results found by various groups that have not taken into account the time frame of hypoxic ROS production. We propose that this acute and transient hypoxia-induced superoxide burst may be translated into oxidative signals contributing to hypoxic adaptation and preconditioning.

In most metazoans, oxygen has to be distributed through the organism to be used by cells within various organs. In several physiological and pathophysiological scenarios, cells undergo a decrease in the amount of available oxygen, known as hypoxia, which induces acute and long-term cellular, local, and systemic responses [1]. Most of the long-term responses are mediated by the induction of over 100 genes by the hypoxia-inducible factors (HIFs), heterodimeric transcription factors composed of a constitutively expressed subunit (HIF-β) and an O_2-dependent HIF-α subunit. In normoxia the latter subunit is continuously degraded through a mechanism mediated by a family of HIF prolyl hydroxylases (EGLNs or PHDs), which carry out an O_2-dependent hydroxylation that is suppressed when oxygen concentration decreases, allowing HIF-α stabilization [2]. Some studies revealed that HIF-α stabilization was associated with an acute increase in reactive oxygen species (ROS) production in hypoxia [3,4].

It has been shown that acute responses to hypoxia involve local temporal changes in redox state due to the alterations in production of short-lived reactive oxygen species [5–8]. However, the nature of oxygen-sensing free radical generators, the targets of these radicals, and the resulting changes in enzyme activity and, finally, whether hypoxia causes a decrease or an increase in ROS production remain a matter of debate. Hypoxia-induced ROS production has been attributed mainly to the mitochondrial oxidative phosphorylation system (OXPHOS) and has been proposed to contribute to PHD inhibition and HIF-α stabilization [9–12] (reviewed in [13,14]).

Abbreviations: 2-OH-E, 2-hydroxyethidium; BAEC, bovine aortic endothelial cell; CDCFDA, 5(6)-carboxy-2′,7′-dichlorofluorescein diacetate; DCF, dichlorofluorescein; DHE, dihydroethidium; HIF, hypoxia-inducible factor; Mito-HE, mito-hydroethidine; OXPHOS, mitochondrial oxidative phosphorylation system; ROS, reactive oxygen species; TMRM, tetramethylrhodamine methyl ester

* Corresponding author. Fax: +34 915202374.
E-mail address: amartinezruiz@salud.madrid.org (A. Martínez-Ruiz).
[1] *Present address:* Departamento de Biología Físico-Química, Centro de Investigaciones Biológicas, CSIC, E-28040 Madrid, Spain.

http://dx.doi.org/10.1016/j.freeradbiomed.2014.03.011
0891-5849/

This posed a paradox, as superoxide is directly produced from oxygen so its production rate should decrease with a decrease in oxygen availability [13,15]. Indeed, some of these findings and methodological approaches have been questioned [16,17] (reviewed in [18]). However, detailed investigations confirmed that increased ROS production occurred under conditions of mild hypoxia (1–3% O_2), but not during severe hypoxia or anoxia [13,19,20].

ROS production in hypoxia has often been measured with fluorescent probes that are oxidized by different species. The main limitation of some (if not most) of these studies is that the fluorescence measurements were performed outside the hypoxia chamber with reoxygenation occurring during the measurements. Several recent reports have confirmed hypoxic ROS production in cells exposed to hypoxia while recording the fluorescent signal from HSP-FRET or roGFP [5,9,21–23] (reviewed in [13,24]). Both thiol-based protein sensors are oxidized by H_2O_2, although oxidation by other intracellular oxidants cannot be ruled out. Superoxide anion is the primary ROS produced by the OXPHOS. However, there are few reports using a specific probe for direct measurement of this species in hypoxic cells [17,20,25] and we are not aware of any study showing the dynamics of superoxide production upon deoxygenation. Understanding the time course of superoxide production will help us approach the mechanisms underlying that response.

By using a novel proteomic method for detecting reversible thiol oxidation (redox fluorescence switch), we have recently shown a specific pattern of proteins in which cysteine thiol residues are reversibly oxidized when endothelial cells are subjected to acute hypoxia for 2 h [8]. This suggests a role for hypoxia-induced ROS production in cell signaling: the increased ROS levels can produce specific oxidative posttranslational modifications that may regulate the HIF pathway or promote other acute responses [8]. We herein present the data on superoxide production directly assessed in the cytosol and in the mitochondria of cells exposed to acute hypoxic challenge, combining different techniques to avoid potential artifacts.

Materials and methods

Cell culture

Bovine aortic endothelial cells (BAECs) were obtained from aortas donated by a local slaughterhouse and isolated as previously described [26]. BAECs were cultured at 37 °C in RPMI 1640 supplemented with 15% heat-inactivated fetal bovine serum (FBS), 100 U/ml penicillin, and 100 μg/ml streptomycin. They were used between passages 3 and 9; endothelial morphology was assessed by visual inspection and by Western blot for endothelial nitric oxide synthase.

EA.hy926 cells (kindly provided by Dr. Cora-Jean S. Edgell, University of North Carolina, NC, USA) were cultured at 37 °C in Dulbecco's modified Eagle medium (DMEM) supplemented with HAT, 10% heat-inactivated FBS, 100 U/ml penicillin, and 100 μg/ml streptomycin

HeLa cells were cultured at 37 °C in DMEM supplemented with 10% heat-inactivated FBS, 100 U/ml penicillin, and 100 μg/ml streptomycin.

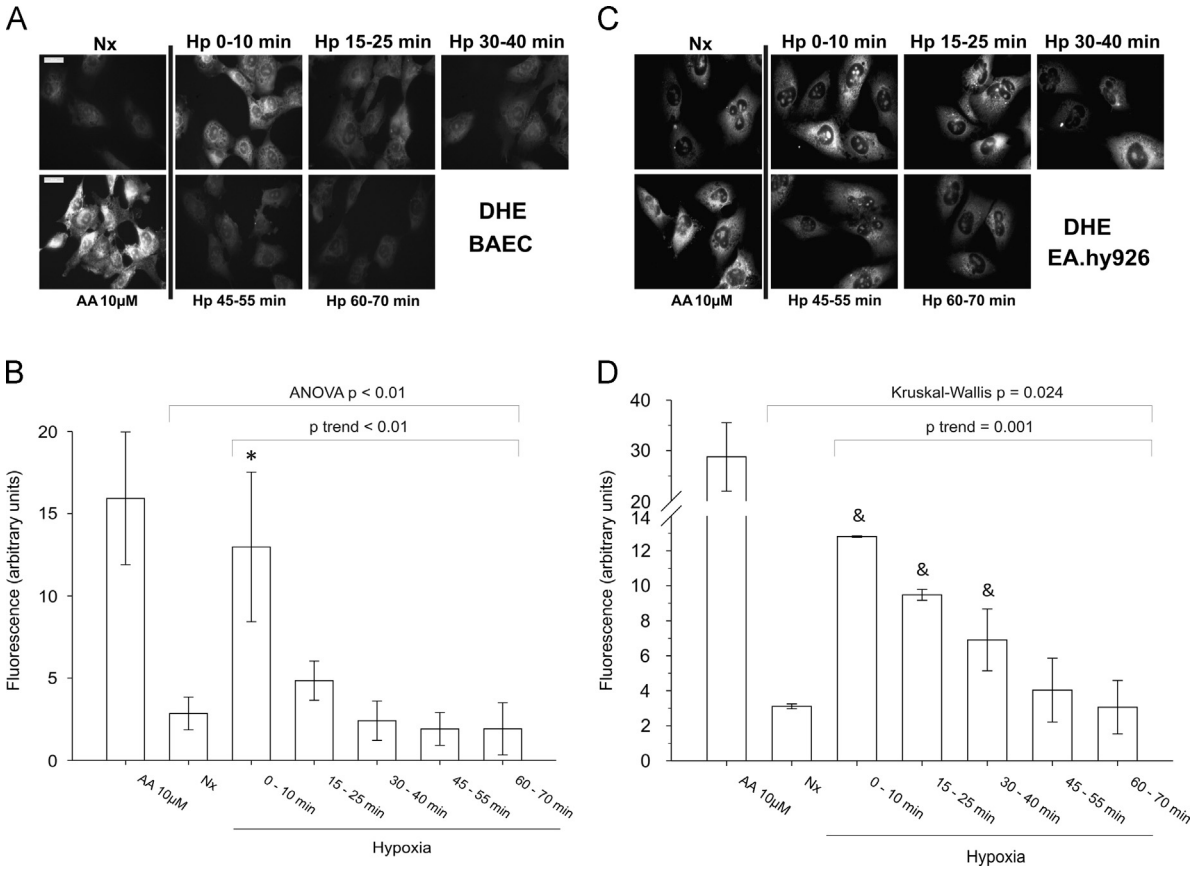

Fig. 1. Superoxide detection by DHE and fluorescence microscopy in fixed endothelial cells. (A, B) BAECs and (C, D) EA.hy926 cells were incubated for 60 min in normoxia (Nx) or in normoxia with antimycin A (AA, 10 μM for 30 min) or incubated in a hypoxia chamber at 1% O_2 with medium preequilibrated in the hypoxic condition (Hp) for 0, 15, 30, 45, or 60 min. 5 μM DHE was added for 10 min more, and the cells were fixed in the hypoxia chamber. (A, C) Representative images showing DHE fluorescence. (B, D) Quantification of images from four (B) or three (D) independent experiments. Data are presented as the mean ± SEM. $^*p < 0.05$, &$p = 0.0495$ versus Nx.

ρ^0L929 cells (mitochondrial DNA-less cells derived from L929 cells) and their control ρ^+ transmitochondrial cybrids, TmC57BL/6J (generated by transferring functional mitochondria from platelets to ρ^0L929 cells), were generated [27] and kindly provided by the group of Dr. José Antonio Enríquez (CNIC, Spain). They were cultured at 37 °C in DMEM supplemented with 5% heat-inactivated FBS, 100 U/ml penicillin, and 100 μg/ml streptomycin. ρ^0L929 cells were also supplemented with 50 μg/ml uridine.

HK-2 cells (kindly provided by Dr. María José Calzada, UAM and Instituto de Investigación Sanitaria Princesa, Madrid, Spain) were cultured at 37 °C in DMEM F-12–GlutaMAX supplemented with 10% heat-inactivated FBS, 100 U/ml penicillin and 100 μg/ml streptomycin, and 0.1% insulin–transferrin–selenium-X solution.

Cardiomyocytes were isolated from rat pups 2–3 days after birth as previously described [28]. The cells were seeded on collagen-coated six-well plates, supplemented with maintenance medium containing 1 part M199 medium and 4 parts medium containing (in mM) 116 NaCl, 32.1 $NaHCO_3$, 1 NaH_2PO_4 (pH 7.2), 0.8 $MgSO_4$, 5.5 glucose, 1.8 $CaCl_2$, supplemented with 1% horse serum, penicillin, streptomycin, and 2% glutamine. Cells were maintained in cell culture incubators (95% air, 5% CO_2 in gas phase, 37 °C) and used within 5 days of isolation.

Fluorescence microscopy in fixed cells and quantification

Cells were seeded a day before experimentation on glass coverslips. For treatments in hypoxia, all the solutions were preequilibrated to hypoxic conditions before use; in some experiments, 1 mM Tiron (4,5-dihydroxy-1,3-benzene disulfonic acid) was added 30 min before experimentation and maintained during the rest of the experiment. Plated cells were introduced in an Invivo2 400 workstation (Ruskinn) set at 1% O_2 (2% O_2 when stated), 5% CO_2, 37 °C, and incubated for the indicated times (0, 15, 30, 45, and 60 min) in new medium, washed three times with Hanks' balanced salt solution with Ca^{2+}/Mg^{2+} (HBSS + Ca/Mg) and incubated with 5 μM mito-hydroethidine (Mito-HE; 3.33 or 10 μM when stated) or 5 μM dihydroethidium (DHE) for 10 min, or with 10 μM 5(6)-carboxy-2′,7′-dichlorofluorescein diacetate (CDCFDA) for 15 min (all probes in HBSS + Ca/Mg), in darkness. After incubation, excess probe was washed away three times with HBSS + Ca/Mg, and the cells were fixed by adding 4% paraformaldehyde and incubated in darkness at 4 °C for 15 min. After fixation, wells were again washed three times with HBSS + Ca/Mg and coverslips placed on slides. In normoxic cells, medium was also changed for new normoxic medium and treated as hypoxic cells, but in a standard cell incubator. When normoxia was set at 7% O_2, the cells were placed in an Invivo2 200 workstation (Ruskinn) at 7% O_2, 5%

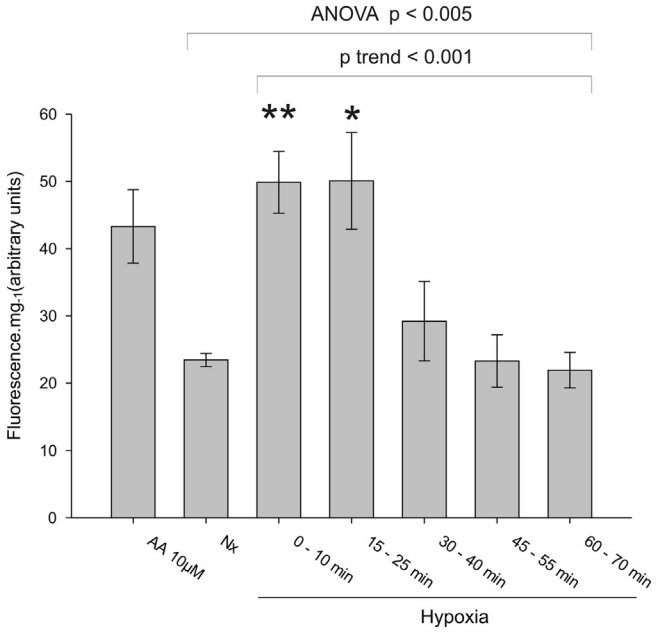

Fig. 2. Superoxide detection by DHE and HPLC in endothelial cells. BAECs were treated as in Fig. 1. After DHE incubation (5 μM DHE, 10 min) cells were lysed in the hypoxia chamber and frozen, and 2-OH-E amount was analyzed by HPLC with fluorescence detection. Data are presented as the mean ± SEM of four independent experiments. $^*p < 0.05$, $^{**}p < 0.01$ versus Nx.

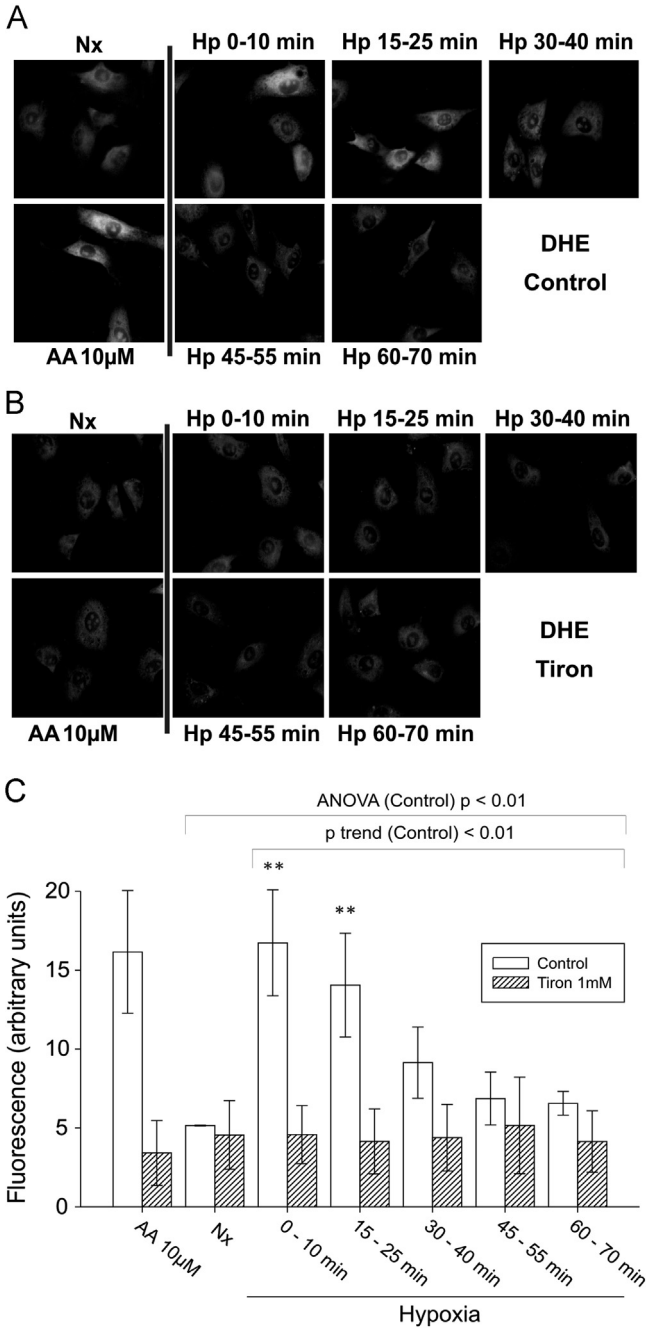

Fig. 3. Superoxide detection by DHE and fluorescence microscopy in fixed endothelial cells treated with 1 mM Tiron. (A) Control BAECs and (B) BAECs incubated with 1 mM Tiron were treated as in Fig. 1. (A, B) Representative images showing DHE fluorescence. (C) Quantification of images from three independent experiments. Data are presented as the mean ± SEM. $^{**}p < 0.01$ versus Nx.

CO_2, 37 °C, incubated overnight, and treated in the same chamber or transferred to the Invivo2 400 chamber for 1% O_2 hypoxia as above. Antimycin A was added to a final concentration of 10 μM onto normoxic cells 30 min before and during incubation with the probe. Three images per coverslip were taken in a Leica DMR fluorescence microscope with a 63× objective, using the following excitation/emission filter pairs: 546-12/560 for DHE and Mito-HE, 480-40/505 for CDCFDA. The images (three images per coverslip; the number of independent experiments is described in the figure legends) were quantified using ImageJ software. The same threshold was set for all the images and the mean value from the histogram was averaged for the three images of each coverslip.

Significance of the hypoxia-induced changes was analyzed using analysis of variance (ANOVA) for normoxic and all the hypoxic time groups, and intergroup comparison was done by the multiple comparison test (Dunnett posteriori test with respect to the normoxia group). The change in fluorescence with the time in hypoxia was evaluated by linear trend test of all the hypoxia groups [29]. Homoscedasticity was tested with Levene's test and normality with the Shapiro–Wilk test. Appropriate transformation was done to perform the analysis in the case of no normal distribution. When no transformation gave normal distribution (Figs. 1D and 6D), nonparametric tests were used: differences among normoxic and all the hypoxic time groups were analyzed with the Kruskal–Wallis test and intergroup comparison was done with the Mann–Whitney test with respect to the normoxia group; the change in fluorescence with the time in hypoxia was evaluated by nonlinear trend test of all the hypoxia groups. All analyses were performed using Stata version 11 software and R version 2.15.2, with the help of the Methodology Unit of the Instituto de Investigación Sanitaria Princesa (Madrid, Spain).

Colocalization analysis of Mito-HE by confocal microscopy

Cells were seeded a day before experimentation on glass coverslips. Plated cells were washed three times with HBSS + Ca/Mg and incubated with 5 μM Mito-HE for 10 min in darkness. After incubation, excess probe was washed away three times with HBSS + Ca/Mg, and the cells were fixed by adding 4% paraformaldehyde and incubated in darkness at room temperature (RT) for 10 min. After fixation, wells were again washed with HBSS + Ca/Mg and cells permeabilized with 0.5% Triton in phosphate-buffered saline (PBS) for 10 min at RT. Blocking solution, consisting in 5-thio-2-nitrobenzoic acid in PBS, was added for 20 min at 37 °C, and antibody against prohibitin-1 C-term (AJ1656a; Abgent) was incubated for 1 h at 37 °C. Coverslips were washed three times with 0.1% Tween 20 in PBS (PBS-T) and incubated with DyLight-488-labeled goat anti-rabbit secondary antibody for 30 min at 37 °C. Cells were washed three times with PBS-T and once with distilled water and coverslips mounted in slides. Tri-color Z stacks were generated using a Leica SP-5 confocal microscope. Samples were excited with an Ar/Kr laser using the 488 nm line and a second diode laser fitted with a 561 nm line. Fluorescence

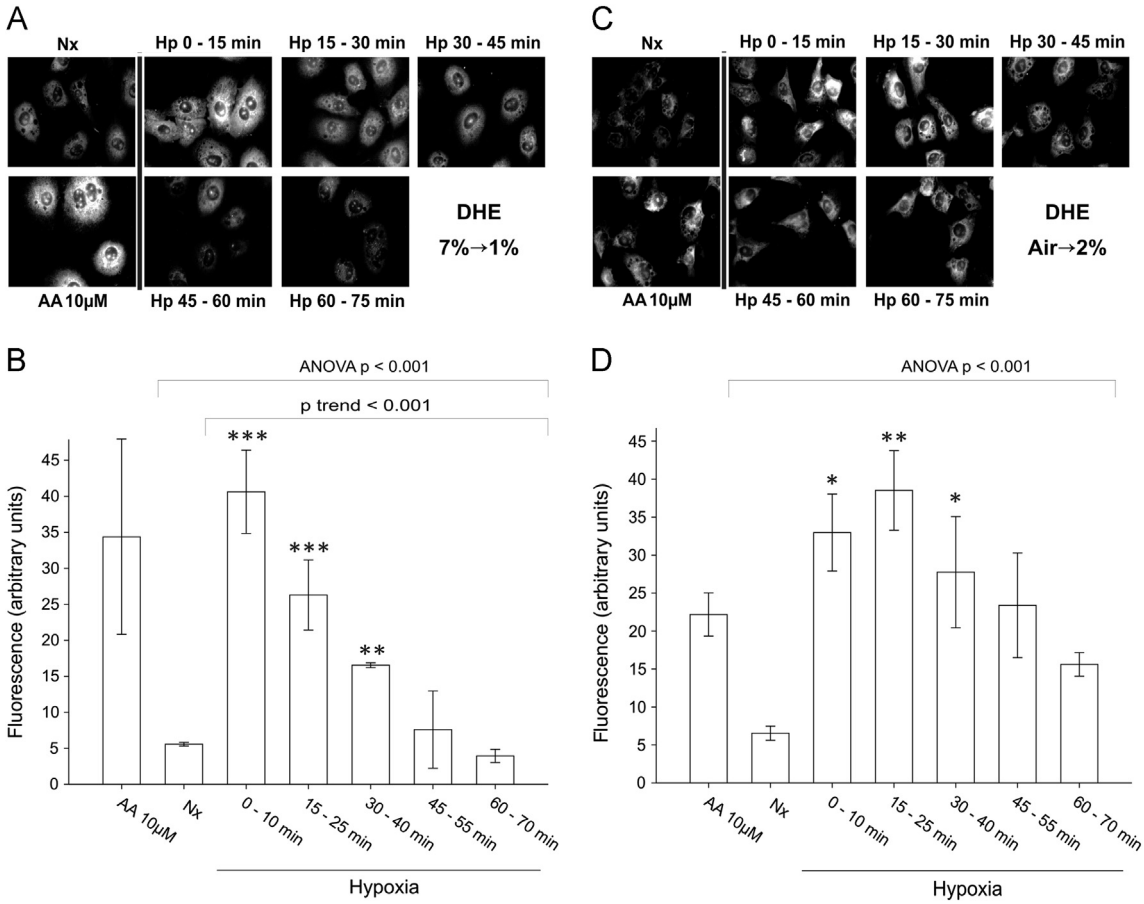

Fig. 4. Superoxide detection by DHE in endothelial cells at different concentrations of O_2 in normoxia and hypoxia. (A, B) BAECs were treated as in Fig. 1, but normoxia was set at 7% O_2. (C, D) BAECs were treated as in Fig. 1, but the hypoxia chamber was set at 2% O_2 and normoxia performed at atmospheric O_2 concentration. (A, C) Representative images showing DHE fluorescence. (B, D) Quantification of images from three independent experiments. Data are presented as the mean ± SEM. $^{***}p < 0.001$ versus Nx, $^{**}p < 0.01$ versus Nx, $^{*}p < 0.05$ versus Nx.

emission was taken using the spectral capability of the SP-5 according to the manufacturer's instructions. For three-dimensional analysis, stacks were processed using ImageJ software.

High-performance liquid chromatography (HPLC) analysis

Cells were seeded a day before experimentation in 60-mm-diameter plates. For hypoxia treatments, plated cells were introduced into an Invivo2 400 workstation (Ruskinn) set at 1% O_2, 5% CO_2, 37 °C, and incubated for the indicated times (0, 15, 30, 45, and 60 min) in prehypoxic medium, washed three times with prehypoxic HBSS + Ca/Mg and incubated with 5 μM DHE for 10 min (in prehypoxic HBSS + Ca/Mg solution), in the darkness. After incubation, excess probe was washed away once with prehypoxic PBS and cells were lysed with 0.1% Triton X-100 and frozen overnight at −80 °C. Homogenates were thawed on ice and 100 μl was transferred into a new tube. 1-butanol (250 μl) was added to the lysate, vortexed for 1 min, and centrifuged for 3 min at maximum speed and the upper alcoholic phase was recovered and dried. The desiccated fraction was resuspended in 100 μl HPLC-grade water and vortexed. An HPLC 2695 separation module from Waters was used to load and separate 50 μl of the samples in a Mediterranean Sea C18 column using acetonitrile 10%–trifluoroacetic acid (TFA) 0.1% and acetonitrile 100%–TFA 0.1% as mobile phases. Fluorescence of the samples was detected by a W474 module at 490 nm excitation wavelength and 560 nm emission wavelength. The peak area corresponding to hydroxyethidium formation was quantified and corrected with the protein concentration of the sample (determined by the BCA assay). Statistical analysis was performed as for fluorescence microscopy in fixed cells (see above).

Live imaging fluorescence microscopy and quantification

Cells were seeded in six-well plates a day before experimentation. Plated cells were washed three times with HBSS + Ca/Mg and incubated with 5 μM Mito-HE, 10 μM DHE, 30 nM tetramethylrhodamine methyl ester (TMRM), or 10 μM CDCFDA for 20 min at 37 °C in darkness. After that the plate was placed in a Leica DM 16000B fluorescence microscope equipped with a Leica DFC360FX camera, an automated stage for live imaging, and a thermostated hypoxic cabinet. The planes were focused for image capture, and images were taken with a 20× objective every 2 min for 40 min, providing a total of 20 cycles. Normoxia experiments started and ended at 20% O_2 and 5% CO_2, whereas hypoxia experiments started at 20% O_2 and 5% CO_2 and were switched to 2% O_2 and 5% CO_2 in cycle 2. The excitation/emission filter pairs used were 546-12/560 for DHE, Mito-HE, and TMRM, 480-40/505 for CDCFDA.

For mitochondrial membrane potential controls, 12.5 μM oligomycin or 1 μM carbonyl cyanide-4-(trifluoromethoxy)phenylhydrazone (FCCP) were added before focusing the planes.

Images were quantified with Leica Las-AF software. Three independent experiments were performed for each condition. For each experiment and condition, four identical linear regions of interest (ROIs) were created on nonnuclear regions of different cells (to avoid measuring nuclear binding of Mito-HE and DHE). The maximum peak value of cycles 0, 5, 10, 15, and 20 was collected for each ROI. The oxidation rate for each replicate was estimated by linear regression of the data for all the ROIs and time points. The differences in the means of the replicate oxidation rates were analyzed by the Student *t* test. Homoscedasticity was tested with Levene's test and normality with the Shapiro–Wilk test. Appropriate transformation was done to perform the analysis in the case of no homoscedasticity or no normal distribution. These statistical analyses were performed using G-Stat version 2.0.1 software.

Treatment effect was analyzed with GEE (generalized estimating equations method) with Gaussian family and identity link function [30]. Variability of statistics derived from time observations was analyzed with independent and autoregressive of order 1 (AR1)—correlation structures [30]. However, only the independent correlation structure is shown for the within-subject correlation, because it was the most parsimonious model (*p* value and coefficient were similar between the two structures, therefore the statistical independence of observations could be assumed). This independent correlation structure is equal to simple regression models. When the response variables were not normally distributed appropriate transformations were used. These analyses were performed using Stata version 12 software with the help of the Methodology Unit of the Instituto de Investigación Sanitaria Princesa (Madrid, Spain).

Western blot analysis

Protein extracts were run on 10% standard polyacrylamide gel electrophoresis and transferred to nitrocellulose membranes. Monoclonal anti-HIF-1α antibody (MAB1536; R&D Systems) and monoclonal anti-α-tubulin antibody (T6199; Sigma) were used. Antibody binding was detected by chemiluminescence with species-specific secondary antibodies labeled with horseradish peroxidase and visualized on a digital luminescence image analyzer (Fujifilm LAS-4000).

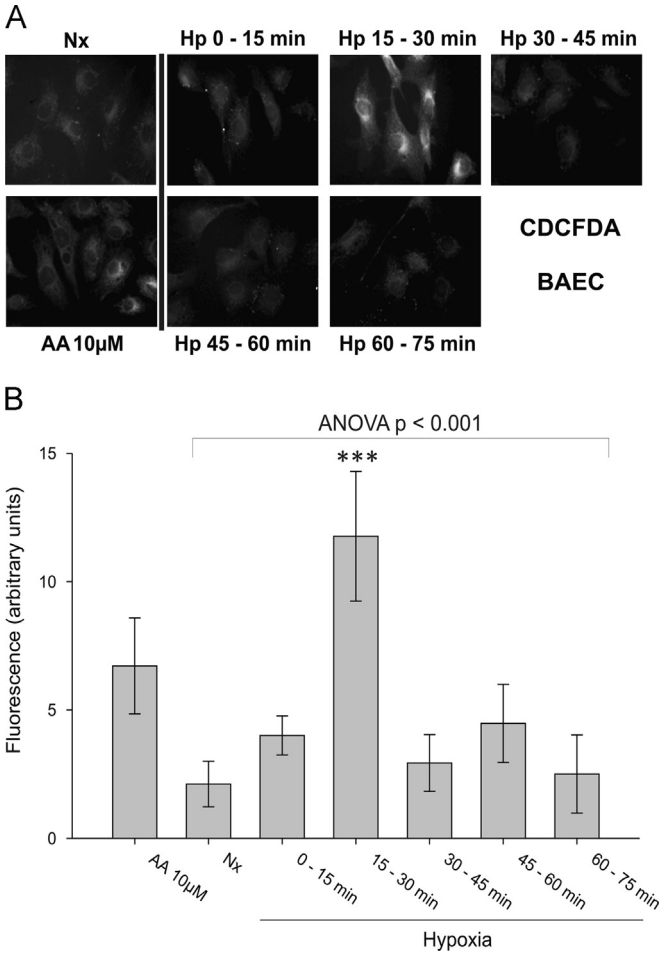

Fig. 5. ROS detection by CDCFDA and fluorescence microscopy in fixed endothelial cells. BAECs were treated as in Fig. 1. CDCFDA 10 μM was added for 15 min more, and cells were fixed in the hypoxia chamber. (A) Representative images showing CDCFDA fluorescence. (B) Quantification of images from four independent experiments. Data are presented as the mean ± SEM. $^{***}p < 0.001$ versus Nx.

Results and discussion

Hypoxia induces a superoxide burst in the first minutes of hypoxia in endothelial cells

We aimed to determine whether reduction in oxygen concentration was able to induce the production of superoxide ($O_2^{\bullet-}$) at different times. DHE reacts with superoxide to produce 2-hydroxyethidium (2-OH-E), which can be detected by fluorescence microscopy. As a positive control we used antimycin A, which inhibits complex III of the OXPHOS system, increasing superoxide production [31]. Primary BAECs were subjected to hypoxia for various times, ranging from 10 to 70 min. DHE was added over the last 10 min of hypoxic exposure, and after that, the cells were fixed in the hypoxia chamber. The amount of 2-OH-E produced was assessed in a fluorescence microscope (Fig. 1A and B). Compared to the measure in normoxia, a significant increase in superoxide production was observed within the first minutes of hypoxia. An additional analysis of the linear trend (*p* trend [29]) among the measures at various times in hypoxia showed that superoxide production was progressively diminished over the following hour. Similar results were obtained with a cell line derived from human endothelial cells, EA.hy926 [32] (Fig. 1C and D).

DHE oxidation measurement by fluorescence microscopy is not completely specific for superoxide detection, as there are other reactions that can also give fluorescent products, but 2-OH-E can be differentiated from ethidium and other products by HPLC analysis with fluorescence detection [33]. To confirm the results from microscopy and to unambiguously detect the production of superoxide, we performed HPLC analysis of cell lysates from BAECs subjected to hypoxia, incubated with DHE, and extracted in the hypoxia chamber. The peak of 2-OH-E was clearly separated from the peak of ethidium, both in control experiments with cyclosporin A treatment [34] and in hypoxia treatments (Supplementary Fig. 1). With this methodology we also observed a transient burst of superoxide production during the first minutes of hypoxia (Fig. 2). Superoxide signal thereafter decreased and did not differ from normoxic values after 45–60 min in hypoxia. These findings correlated with the results obtained by fluorescence microscopy (Fig. 1), confirming the specific detection of superoxide in our setting.

To further confirm the superoxide burst, we aimed to inhibit it with specific reagents, so we treated BAECs with Tiron before and during the hypoxic incubation in microscopy experiments. Tiron reacts with superoxide, and clearly abolished the signal from the superoxide burst in hypoxia (Fig. 3).

To assess if this superoxide burst is specific for the change in oxygen concentrations we have used in the experimental setting, we performed similar experiments with different initial and final oxygen concentrations. First, we used a lower initial "normoxic" reference concentration, 7% O_2, which could be more physiologically relevant for endothelial cells, maintaining the hypoxia at 1% O_2. We observed a similar superoxide burst (Fig. 4A and B). A similar increase in superoxide production was observed when 2% O_2 was used as hypoxia and ambient air was used as normoxia. In fact the amplitude of the superoxide burst at 2% O_2 exceeded that observed at 1% O_2 (Fig. 4C and D).

To determine the production of H_2O_2 (along with $ONOO^-$ and other ROS [35]) that could be derived from the superoxide burst we used CDCFDA. BAECs incubated in hypoxia showed a burst in

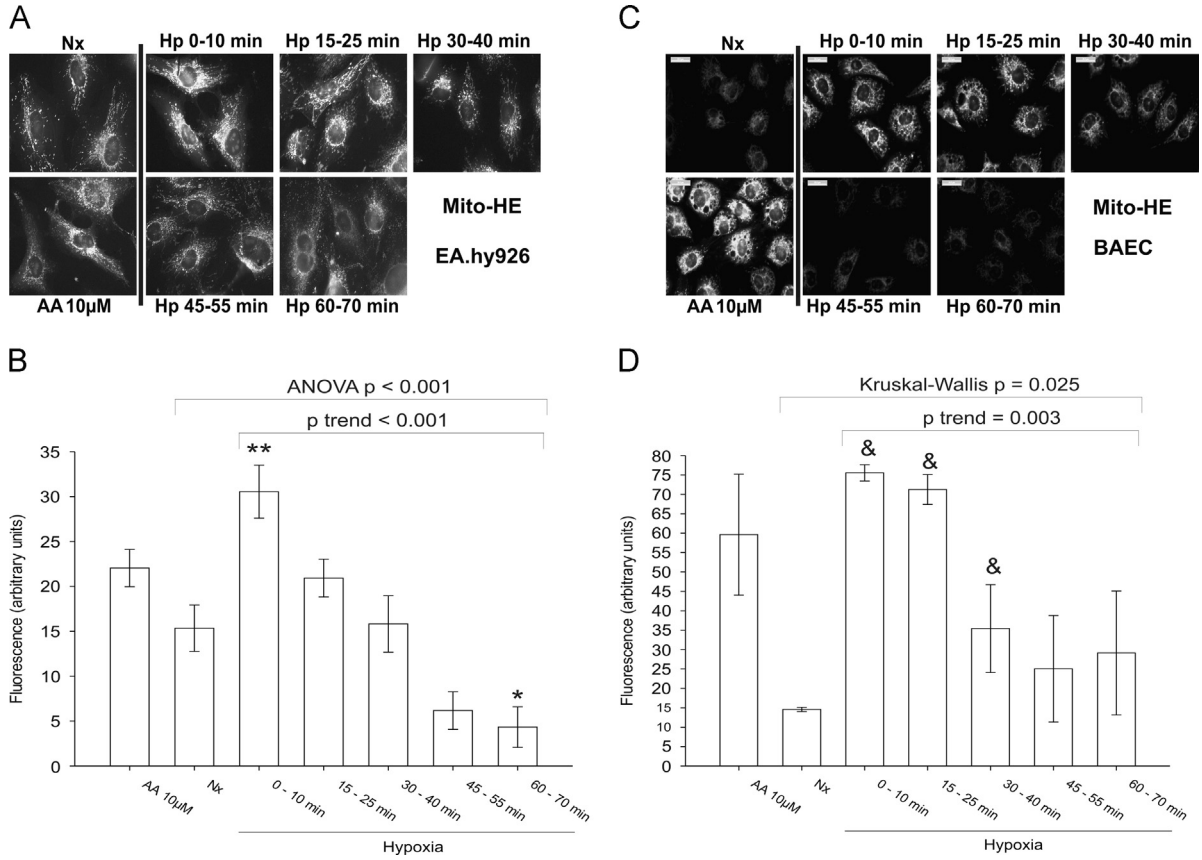

Fig. 6. Mitochondrial superoxide detection by Mito-HE and fluorescence microscopy in fixed endothelial cells. (A, B) EA.hy926 cells and (C, D) BAECs were treated as in Fig. 1. Mito-HE 5 μM was added for 10 min more, and the cells were fixed in the hypoxia chamber. (A, C) Representative images showing Mito-HE fluorescence. (B, D) Quantification of images from three independent experiments. Data are presented as the mean ± SEM. $^*p < 0.05$, $^{**}p < 0.01$, &$p = 0.0495$ versus Nx.

CDCFDA oxidation, which peaks at 15–30 min (Fig. 5), suggesting that the superoxide burst is translated into a burst of other ROS such as H_2O_2 with a slight delay. A similar kinetics has been described for CDCFDA oxidation after VEGF addition, increased under hypoxic conditions [36].

Superoxide is produced in mitochondria

We next wanted to explore the role of mitochondria in hypoxia-induced superoxide production. To this end, we used the mitochondria-targeted probe Mito-HE, in which a triphenylphosphonium (TPP^+) group is linked to DHE. Mito-HE accumulates within active mitochondria because positively charged TPP^+ drives the compound to the negatively charged mitochondrial matrix. EA.hy926 cells incubated with Mito-HE during the last 10 min of exposure to 1% O_2 showed a similar acute transient rise in superoxide production in response to hypoxia (Fig. 6A and B), suggesting mitochondrial localization of superoxide production. Again, similar results were obtained in BAECs, in which superoxide production in hypoxia could be even higher (Fig. 6C and D).

We confirmed mitochondrial targeting of Mito-HE by assessing colocalization with prohibitin-1, a mitochondrial protein (Supplementary Fig. 2A) [37]. To additionally control that the Mito-HE signal was actually related to increases in superoxide production and there was no saturation effect in the signal, we tested different concentrations of Mito-HE, observing that there is a clear increase with the Mito-HE concentration (Supplementary Fig. 2B).

A complementary approach to analyzing the mitochondrial origin of the superoxide production came from the study of the hypoxia response in ρ^0 cells, which do not have a functional OXPHOS owing to mitochondrial DNA damage. ρ^0 cells (ρ^0L929) and their control cybrids with undamaged mitochondria (TmC57BL/6J, from now on called C57) [27] were subjected to hypoxia and DHE fluorescence was measured under the same conditions as with endothelial cells. C57 cells also showed a superoxide burst in the first minutes of hypoxia (Fig. 7). However, ρ^0L929 cells showed much lower DHE signal, which did not increase with antimycin A treatment (owing to the lack of OXPHOS); hypoxic exposure of ρ^0L929 cells also did not significantly affect the DHE (Fig. 7). In line with the previous data these findings point also to the mitochondrial origin of the superoxide burst that we observe in the first minutes of hypoxia.

Early hypoxic superoxide production is confirmed in living cells

In the previous experiments the accumulation of ROS was detected over the 10 or 15 min after 0–60 min of incubation under hypoxic or normoxic conditions. To get a complementary measure of ROS production in hypoxia, we monitored the rates of oxidation of the ROS-sensitive probes using live imaging under normoxic or hypoxic conditions. Under normoxic conditions a gradual sustained increase in the oxidation signal was detected in BAECs using DHE, Mito-HE, and CDCFDA (Fig. 8A–C). In these experiments, the fluorescent signal accumulated over time because of the irreversible oxidative modification of the probes. Thus, this method allowed assessing only the change in the rate of oxidation, which reflects the relative changes in differences in ROS production, and not the differences between the time points. We confirmed a significant increase in the rate of ROS production in BAECs for all the three probes when cells were subjected to hypoxia (Fig. 8A–C).

Using live imaging we also explored the oxygen-dependent changes in the mitochondrial membrane potential. Mitochondrial targeting of Mito-HE is driven by mitochondrial membrane potential. Thus, hyperpolarization is associated with greater accumulation of Mito-HE within mitochondria and a concomitant increase in fluorescence, which is not caused by increased superoxide formation. We measured the mitochondrial membrane potential in BAECs using TMRM in nonquenching mode [38], confirmed by the clear and immediate decrease in the signal when FCCP (which depolarizes the membrane by uncoupling OXPHOS) was added and the increase after addition of oligomycin (which inhibits ATPase, increasing the potential) (Supplementary Fig. 3). Hypoxic treatment of BAECs was associated with mitochondrial depolarization, whereas the potential was maintained in BAECs in normoxia (Fig. 8D). Thus, superoxide production in the mitochondria of hypoxic BAECs could be underestimated using

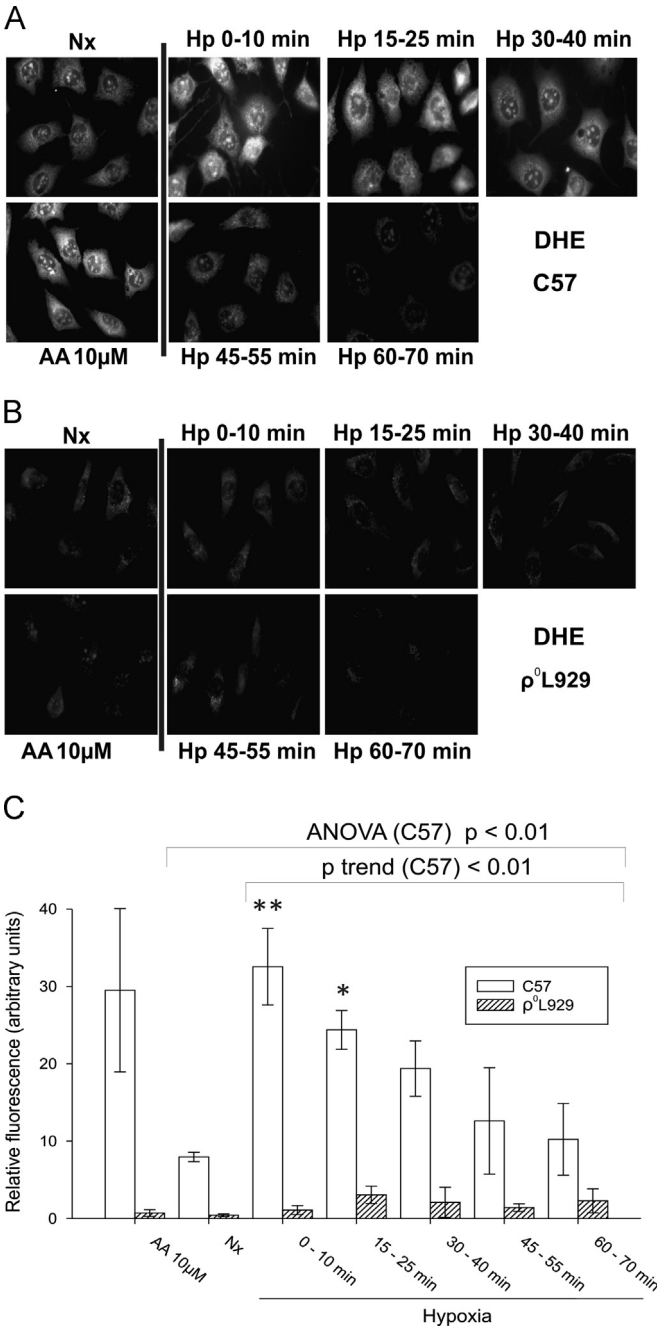

Fig. 7. Superoxide detection by DHE and fluorescence microscopy in fixed C57 and ρ^0L929 cells. (A) C57 and (B) ρ^0L929 cells were treated as in Fig. 1. (A, B) Representative images showing DHE fluorescence. (C) Quantification of images from three independent experiments. Data are presented as the mean ± SEM. $^{**}p < 0.05$, $^{*}p < 0.01$ versus Nx.

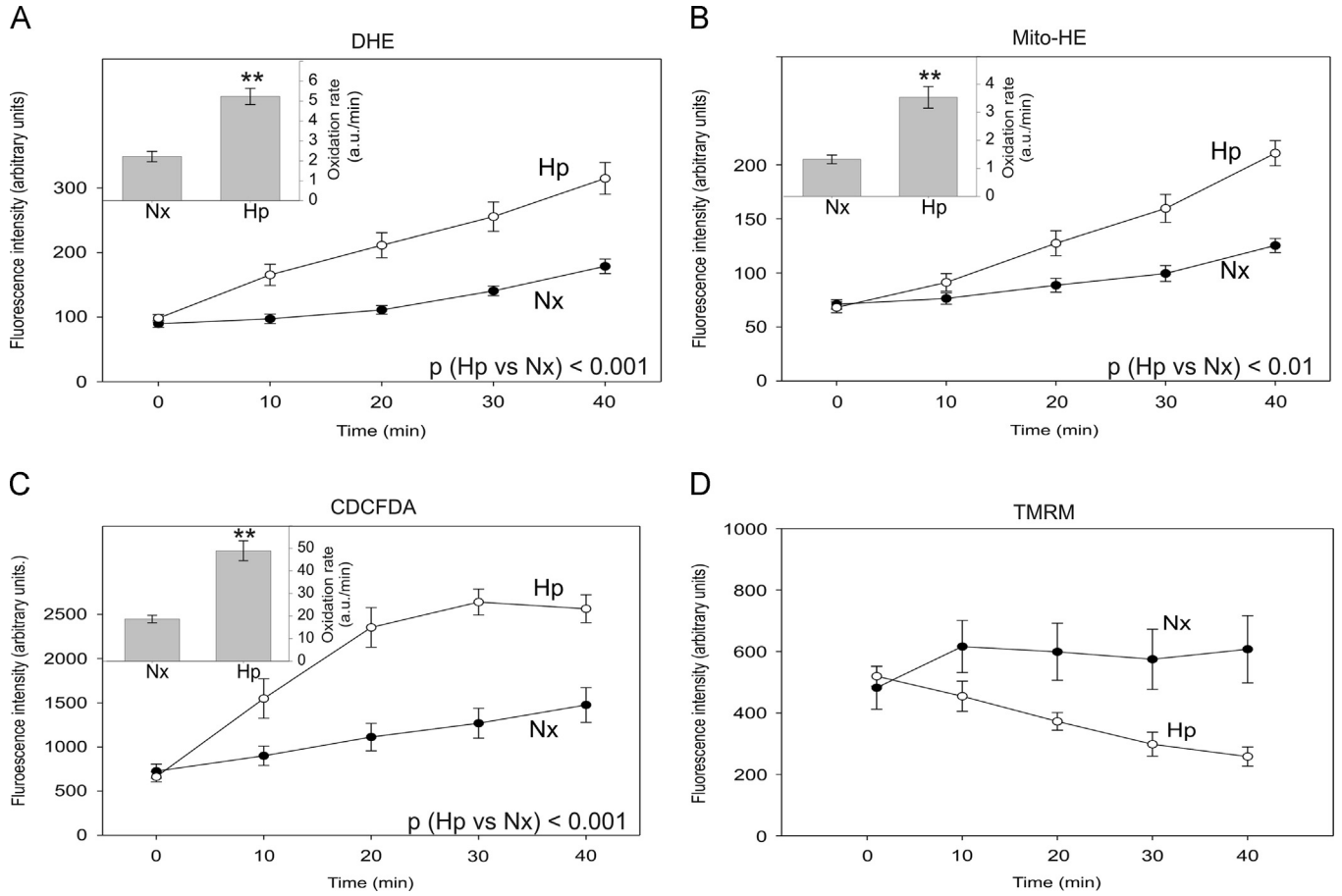

Fig. 8. Superoxide, ROS, and mitochondrial membrane potential measurement by fluorescence microscopy in live endothelial cells. BAECs were incubated with (A) 10 μM DHE, (B) 5 μM Mito-HE, (C) 15 μM CDCFDA, or (C) 30 nM TMRM for 20 min and subsequently incubated in a chamber with atmospheric and temperature control in a fluorescence microscope, where they were maintained in normoxia or subjected to 2% O_2 for 40 min. Quantification of four regions for three independent experiments is plotted for each time as the mean ± SEM. Black circles, normoxia (Nx); white circles, hypoxia (Hp). The *p* value shown corresponds to the evaluation of the treatment effect evaluated with the GEE method with independent correlation structure. (Insets in A–C) Oxidation rates considering all time points of each replicate ($n = 3$) are plotted as the mean ± SEM. $^{**}p < 0.01$ versus Nx.

Mito-HE, as the dye levels in depolarized hypoxic mitochondria would be lower than in the mitochondria of normoxic cells.

Live imaging also confirmed the mitochondrial implication in the increased superoxide production in hypoxia. Whereas C57 cells exhibit a clear increase in the DHE and CDCFDA signals when they are subjected to hypoxia, ρ^0L929 cells do not show these changes when subjected to hypoxia (Fig. 9).

Superoxide burst and ROS formation in hypoxia are not specific solely to endothelial cells

We wondered whether the hypoxia-induced superoxide burst and the increase in ROS production were specific to endothelial cells or a common feature for several cell types, in addition to the fibroblasts previously shown (Figs. 7 and 9). We carried out live imaging experiments with cultured neonatal rat cardiomyocytes. In line with the results obtained in endothelial cells, hypoxia triggered a significant increase in the rate of oxidation of DHE, Mito-HE, and CDCFDA, indicating an increased production of ROS (Fig. 10A–C). Furthermore, depolarization of the mitochondrial membrane in hypoxic cardiomyocytes was confirmed when monitoring signal intensity of TMRM (Fig. 10D), suggesting that superoxide production within mitochondria could be underestimated.

We also assessed whether tumor cells could exhibit a similar response to hypoxia. HeLa and HK2 cells were exposed to acute hypoxia and incubated with Mito-HE at different times (Supplementary Figs. 4 and 5). The response was similar to that of endothelial cells, thus reinforcing the involvement of mitochondria in hypoxic superoxide production and suggesting that this could represent a general mechanism for various cell types.

Superoxide burst as a regulator of HIF-1α stability

As previously stated, hypoxic ROS production has been implicated in triggering hypoxia adaptation signals through the HIF pathway, mediated by HIF-α subunit stabilization [13,14]. Additionally, we have recently shown that in endothelial cells there is a reversible oxidation in certain proteins after 2 h of hypoxia, which could be implied in acute responses to hypoxia [8]. Thus, the superoxide burst we observe could take part in hypoxic signals at longer times, related to the different kinetics of accumulation of different oxidized species.

To test this, we studied HIF-1α stabilization in the systems in which we have been able to abolish the superoxide burst in hypoxia, namely ρ^0 cells and treatment with Tiron. In accordance with results published elsewhere for other ρ^0 cells [3,9,10], ρ^0L929 cells did not stabilize HIF-1α in hypoxia as happened in the control C57 cells (Fig. 11A). Contrary to our hypothesis, Tiron treatment in BAECs did not abolish HIF-1α stabilization in hypoxia and even increased it, both in normoxia and in hypoxia (Fig. 11B). Measurement of CDCFDA oxidation showed that cells with Tiron produced equal or slightly higher signals than cells

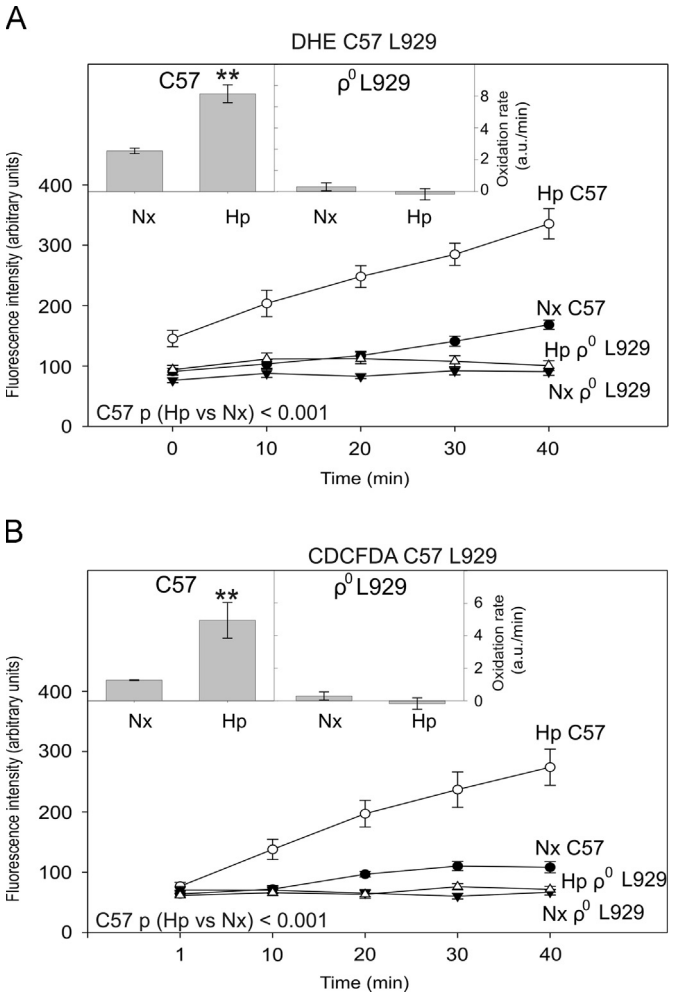

Fig. 9. Superoxide and ROS measurement by fluorescence microscopy in live C57 and ρ^0L929 cells. C57 and ρ^0L929 cells were incubated with (A) 10 μM DHE and (B) 15 μM CDCFDA and treated as in Fig. 8. Quantification of four regions for three independent experiments is plotted for each time as the mean ± SEM. Black circles, C57 in normoxia (Nx C57); white circles, C57 in hypoxia (Hp C57); black inverted triangles, ρ^0L929 in normoxia (Nx ρ^0L929); white triangles, ρ^0L929 in hypoxia (Hp ρ^0L929). The *p* value shown corresponds to the evaluation of the treatment effect evaluated with the GEE method with independent correlation structure. (Insets) Oxidation rates considering all time points of each replicate ($n = 3$) are plotted as the mean ± SEM. $^{**}p < 0.01$ versus Nx.

without treatment (Supplementary Fig. 6); this can be related to the reduction of superoxide due to the reaction with Tiron, producing mainly H_2O_2, which can explain increased HIF-1α stabilization.

Conclusions and future directions

Using several converging methodologies that avoid reoxygenation we have demonstrated that exposure of cells to acute mild hypoxia (1–2% O_2 under our culture conditions) was associated with a burst in superoxide production within the first minutes. Thereafter the levels of superoxide production in hypoxic cells reduced gradually over time. In 1 h no difference in superoxide production could be detected between hypoxic (1% O_2) and normoxic cells. Our results comparing different hypoxic O_2 concentrations in the same experimental setting (Figs. 1, 4C, and 4D) show that at 2% O_2 the superoxide burst can be slower and more sustained than at 1% O_2. These observations resolve the seeming contradiction in the findings reported earlier. For example, Quintero et al. [20] analyzed superoxide production by incubating endothelial cells with DHE for the first 60 min of hypoxia (3% O_2), showing a clear increase in the fluorescence signal; under these conditions, DHE would be oxidized by the superoxide burst that we have seen in our experiments. On the other hand, Chua et al. [17] saw no increase in DHE fluorescence when HEK293 cells were exposed to 1% hypoxia; but in this case DHE was added for 30 min after 3 h of incubation of the cells in hypoxia, which would not allow the detection of the initial superoxide burst.

Other studies have also shown an increase in DHE oxidation in cardiomyocytes in a model of acute ischemia for up to 60 min, in which, in addition to hypoxia, nutrients were removed from the cell culture medium [39]. Further studies would be interesting to evaluate the relative role of oxygen and nutrient depletion, as well as the putative significance of this mechanism in ischemic preconditioning.

We have seen a similar superoxide burst in different types of cells exposed to hypoxia and using either a probe distributed throughout the cell or a mitochondria-targeted probe. When we used ρ^0 cells, lacking a functional OXPHOS, the superoxide burst was abolished. Although we cannot rule out that other mechanisms of superoxide production could be implicated, this strongly suggests that the superoxide burst in the first minutes of hypoxia comes from the mitochondrial OXPHOS system, and it could be related to an early rearrangement of oxygen distribution and the electron transport chain throughout the system. The fact that at 2% O_2 the superoxide production seems to be more intense and prolonged than at 1% O_2 allows speculation that the decrease in superoxide production after some time of hypoxia could be related to a decrease in the O_2 availability inside the mitochondria, which could be delayed with respect to the O_2 reduction outside the cells.

The fact that DCF oxidation was maximal after 15 min of hypoxic exposure suggests that the superoxide burst during the first minutes of hypoxia translates into an increase in H_2O_2 or other ROS with a certain delay in time. This could be related to the different kinetics of accumulation of the diverse ROS, although it can be also an effect of the different probes used or even that the superoxide burst could trigger peroxide generation by other pathways; a more detailed evaluation of this relationship would deserve further investigation. The increase in protein modification by thiol oxidation occurs later on and was observed after 2 h of hypoxia in endothelial cells [8]; in further experiments, we have observed protein thiol oxidation initiating after 30 min of hypoxia in the same setting (unpublished results). If this signal takes part in the stabilization of a transcription factor such as HIF-α, and accumulation of target mRNAs, this could happen at even longer times. Our experiments studying the functional consequences of ablating the superoxide burst on HIF-1α stabilization (Fig. 11) are not fully conclusive. On one hand, although both the superoxide burst and the HIF-1α stabilization were ablated in ρ^0 cells, there could be many other effects related to OXPHOS impairment that could be taking part. On the other hand, Tiron was effective in scavenging superoxide, but probably increased H_2O_2 levels, which correlated with equal or increased HIF-1α stabilization. Thus, further experiments would be needed to assess this, probably with more specific interventions to inhibit the superoxide burst.

We propose that a superoxide production burst in the first minutes, which is translated into cell signals mediated by redox posttranslational modifications, may result in complex responses of the cells to hypoxia (and maybe ischemia) such as adaptation and preconditioning. This may include the activation of the HIF pathway and the concomitant modification of gene expression, although other HIF-independent responses could be triggered by such redox-based signal. Further research in this area should take into account not only the intensity of the hypoxic stimulus and the cell type and context, but also the time frame of the stimuli and of ROS production and signaling.

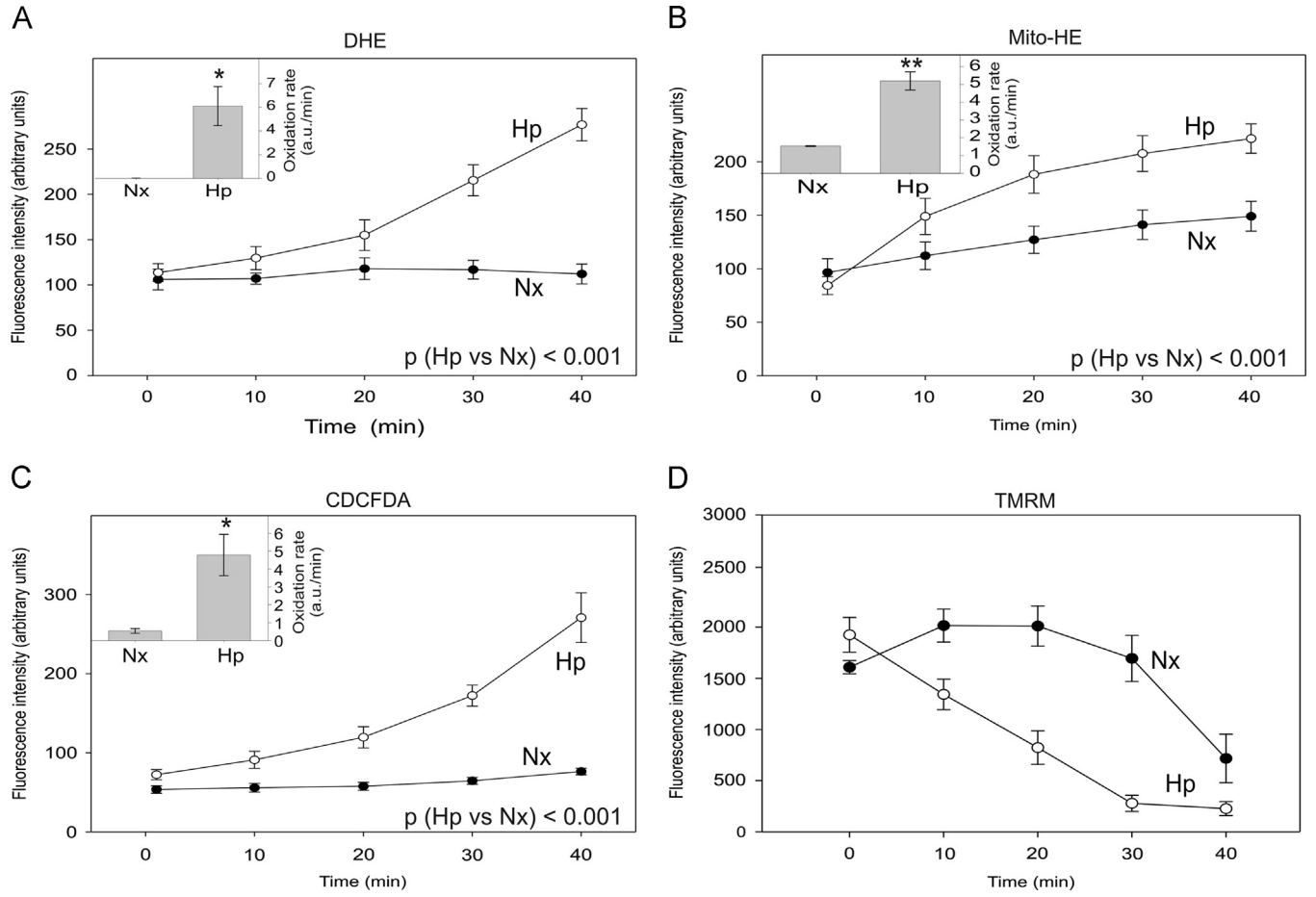

Fig. 10. Superoxide, ROS, and mitochondrial membrane potential measurement by fluorescence microscopy in live cardiomyocytes. Primary cardiomyocytes were treated and data obtained and plotted as in Fig. 8.

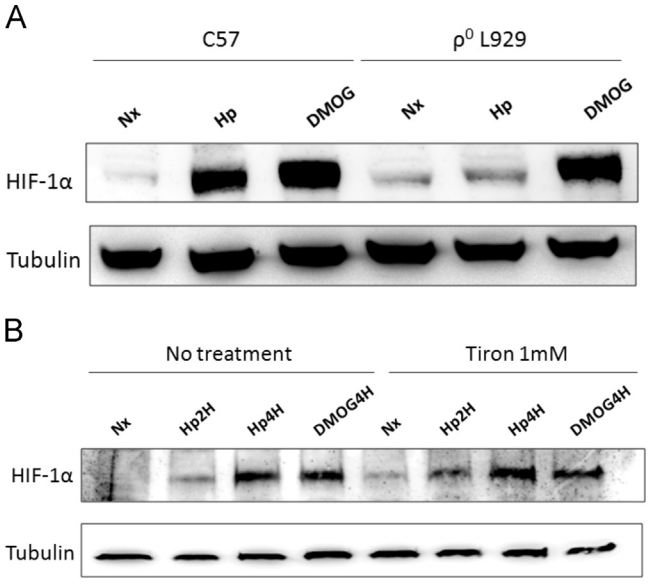

Fig. 11. Immunoblot analysis of HIF-1α in C57 and ρ^0L929 cells and endothelial cells untreated or treated with 1 mM Tiron. (A) C57 and ρ^0L929 cells were exposed for 6 h to normoxia (Nx), normoxia with 1 mM dimethyloxalylglycine (DMOG; a positive control for PHD inhibition and HIF-1α stabilization), or hypoxia (1% O_2, Hp). Proteins were extracted and blotted against HIF-1α protein. Representative image of five independent experiments. (B) BAECs were exposed for 4 h to normoxia (Nx), normoxia with 1 mM DMOG, or hypoxia for 2 (Hp2H) or 4 h (Hp4H). Proteins were extracted and blotted against HIF-1α protein. Representative image of three independent experiments.

Acknowledgments

We thank Lorena Vega Piris and Francisco Rodriguez Salvanés, from the Methodology Unit of the Instituto de Investigación Sanitaria Princesa (IP), for help with statistical analysis and helpful discussions and advice regarding statistics. We thank Dr. Mariusz Kowalewski (Institute of Veterinary Anatomy, UZH) for offering us the microscope to use in our live imaging studies. We thank Dr. José Antonio Enríquez (CNIC, Madrid, Spain), for kindly providing ρ^0 cells and their controls, and Dr. Luis del Peso (UAM, Madrid, Spain) and Dr. Francisco Sánchez-Madrid (IP) for their support. This research has been financed by the Spanish government Grants CSD2007-00020 (RosasNet, Consolider-Ingenio 2010 program; to S.L. and A.M.-R.), CP07/00143 (Miguel Servet program), PS09/00101 and PI12/00875 (to A.M.-R), and SAF2009-7520, SAF 2012-31338, and the "New Indigo" Partnership Program "Nitroxdiab" (PIM2010ENI-00631) (to S.L.); by Swiss National Science Foundation Grant 310030_124970/1 to A.B., by a travel grant from the Instituto de Investigación Sanitaria Princesa (to P.H.-A.); and by the COST actions TD0901 (HypoxiaNet) BM1005 (ENOG–European Network on Gasotransmitters) and BM1203 (EU-ROS). P.H.-A. is the recipient of an FPU fellowship from the Spanish government, and A. M.-R. is supported by the I3SNS program (ISCIII, Spanish government).

Appendix A. Supplementary material

Supplementary data associated with this article can be found in the online version at http://dx.doi.org/10.1016/j.freeradbiomed.2014.03.011.

References

[1] Semenza, G. L. Life with oxygen. *Science* **318:**62–64; 2007.
[2] Kaelin Jr W. G.; Ratcliffe, P. J. Oxygen sensing by metazoans: the central role of the HIF hydroxylase pathway. *Mol. Cell* **30:**393–402; 2008.
[3] Chandel, N. S.; Maltepe, E.; Goldwasser, E.; Mathieu, C. E.; Simon, M. C.; Schumacker, P. T. Mitochondrial reactive oxygen species trigger hypoxia-induced transcription. *Proc. Natl. Acad. Sci. USA* **95:**11715–11720; 1998.
[4] Archer, S. L.; Huang, J.; Henry, T.; Peterson, D.; Weir, E. K. A redox-based O_2 sensor in rat pulmonary vasculature. *Circ. Res.* **73:**1100–1112; 1993.
[5] Desireddi, J. R.; Farrow, K. N.; Marks, J. D.; Waypa, G. B.; Schumacker, P. T. Hypoxia increases ROS signaling and cytosolic $Ca(2+)$ in pulmonary artery smooth muscle cells of mouse lungs slices. *Antioxid. Redox Signaling* **12:**595–602; 2010.
[6] Yakushev, S.; Band, M.; Tissot van Patot, M. C.; Gassmann, M.; Avivi, A.; Bogdanova, A. Cross talk between S-nitrosylation and S-glutathionylation in control of the Na,K-ATPase regulation in hypoxic heart. *Am. J. Physiol. Heart Circ. Physiol.* **303:**H1332–H1343; 2012.
[7] Petrushanko, I. Y.; Yakushev, S.; Mitkevich, V. A.; Kamanina, Y. V.; Ziganshin, R. H.; Meng, X.; Anashkina, A. A.; Makhro, A.; Lopina, O. D.; Gassmann, M.; Makarov, A. A.; Bogdanova, A. S-glutathionylation of the Na,K-ATPase catalytic alpha subunit is a determinant of the enzyme redox sensitivity. *J. Biol. Chem.* **287:**32195–32205; 2012.
[8] Izquierdo-Álvarez, A.; Ramos, E.; Villanueva, J.; Hernansanz-Agustín, P.; Fernández-Rodríguez, R.; Tello, D.; Carrascal, M.; Martínez-Ruiz, A. Differential redox proteomics allows identification of proteins reversibly oxidized at cysteine residues in endothelial cells in response to acute hypoxia. *J. Proteomics* **75:**5449–5462; 2012.
[9] Guzy, R. D.; Hoyos, B.; Robin, E.; Chen, H.; Liu, L.; Mansfield, K. D.; Simon, M. C.; Hammerling, U.; Schumacker, P. T. Mitochondrial complex III is required for hypoxia-induced ROS production and cellular oxygen sensing. *Cell Metab.* **1:**401–408; 2005.
[10] Mansfield, K. D.; Guzy, R. D.; Pan, Y.; Young, R. M.; Cash, T. P.; Schumacker, P. T.; Simon, M. C. Mitochondrial dysfunction resulting from loss of cytochrome c impairs cellular oxygen sensing and hypoxic HIF-[alpha] activation. *Cell Metab.* **1:**393–399; 2005.
[11] Brunelle, J. K.; Bell, E. L.; Quesada, N. M.; Vercauteren, K.; Tiranti, V.; Zeviani, M.; Scarpulla, R. C.; Chandel, N. S. Oxygen sensing requires mitochondrial ROS but not oxidative phosphorylation. *Cell Metab.* **1:**409–414; 2005.
[12] Bell, E. L.; Emerling, B. M.; Ricoult, S. J.; Guarente, L. SirT3 suppresses hypoxia inducible factor 1alpha and tumor growth by inhibiting mitochondrial ROS production. *Oncogene* **30:**2986–2996; 2011.
[13] Guzy, R. D.; Schumacker, P. T. Oxygen sensing by mitochondria at complex III: the paradox of increased reactive oxygen species during hypoxia. *Exp. Physiol.* **91:**807–819; 2006.
[14] Hamanaka, R. B.; Chandel, N. S. Mitochondrial reactive oxygen species regulate hypoxic signaling. *Curr. Opin. Cell Biol.* **21:**894–899; 2009.
[15] Murphy, M. P. How mitochondria produce reactive oxygen species. *Biochem. J.* **417:**1–13; 2009.
[16] Vaux, E. C.; Metzen, E.; Yeates, K. M.; Ratcliffe, P. J. Regulation of hypoxia-inducible factor is preserved in the absence of a functioning mitochondrial respiratory chain. *Blood* **98:**296–302; 2001.
[17] Chua, Y. L.; Dufour, E.; Dassa, E. P.; Rustin, P.; Jacobs, H. T.; Taylor, C. T.; Hagen, T. Stabilization of hypoxia-inducible factor-1alpha protein in hypoxia occurs independently of mitochondrial reactive oxygen species production. *J. Biol. Chem.* **285:**31277–31284; 2010.
[18] Hagen, T. Oxygen versus reactive oxygen in the regulation of HIF-1alpha: the balance tips. *Biochem. Res. Int.* **2012:**436981; 2012.
[19] Schroedl, C.; McClintock, D. S.; Budinger, G. R. S.; Chandel, N. S. Hypoxic but not anoxic stabilization of HIF-1alpha requires mitochondrial reactive oxygen species. *Am. J. Physiol. Lung Cell. Mol. Physiol.* **283:**L922–L931; 2002.
[20] Quintero, M.; Colombo, S. L.; Godfrey, A.; Moncada, S. Mitochondria as signaling organelles in the vascular endothelium. *Proc. Natl. Acad. Sci. USA* **103:**5379–5384; 2006.
[21] Robin, E.; Guzy, R. D.; Loor, G.; Iwase, H.; Waypa, G. B.; Marks, J. D.; Hoek, T. L. V.; Schumacker, P. T. Oxidant stress during simulated ischemia primes cardiomyocytes for cell death during reperfusion. *J. Biol. Chem.* **282:**19133–-19143; 2007.
[22] Iwase, H.; Robin, E.; Guzy, R. D.; Mungai, P. T.; Vanden Hoek, T. L.; Chandel, N. S.; Levraut, J.; Schumacker, P. T. Nitric oxide during ischemia attenuates oxidant stress and cell death during ischemia and reperfusion in cardiomyocytes. *Free Radic. Biol. Med.* **43:**590–599; 2007.
[23] Waypa, G. B.; Marks, J. D.; Guzy, R.; Mungai, P. T.; Schriewer, J.; Dokic, D.; Schumacker, P. T. Hypoxia triggers subcellular compartmental redox signaling in vascular smooth muscle cells. *Circ. Res.* **106:**526–535; 2010.
[24] Schumacker, P. T. Lung cell hypoxia: role of mitochondrial reactive oxygen species signaling in triggering responses. *Proc. Am. Thorac. Soc.* **8:**477–484; 2011.
[25] Yang, W.; Block, E. R. Effect of hypoxia and reoxygenation on the formation and release of reactive oxygen species by porcine pulmonary artery endothelial cells. *J. Cell. Physiol.* **164:**414–423; 1995.
[26] Navarro-Antolín, J.; Rey-Campos, J.; Lamas, S. Transcriptional induction of endothelial nitric oxide gene by cyclosporine A: a role for activator protein-1. *J. Biol. Chem.* **275:**3075–3080; 2000.
[27] Moreno-Loshuertos, R.; Acín-Pérez, R.; Fernández-Silva, P.; Movilla, N.; Pérez-Martos, A.; Rodríguez de Córdoba, S.; Gallardo, M. E.; Enríquez, J. A. Differences in reactive oxygen species production explain the phenotypes associated with common mouse mitochondrial DNA variants. *Nat. Genet.* **38:**1261–1268; 2006.
[28] Rothen-Rutishauser, B. M.; Ehler, E.; Perriard, E.; Messerli, J. M.; Perriard, J. C. Different behaviour of the non-sarcomeric cytoskeleton in neonatal and adult rat cardiomyocytes. *J. Mol. Cell. Cardiol.* **30:**19–31; 1998.
[29] Armitage, P.; Berry, G.; Matthews, J. *Statistical Methods in Medical Research*. Oxford: Blackwell Sci.; 2002.
[30] Hardin, J. W.; Hilbe, J. M. *Generalized Estimating Equations*. Boca Raton, FL: Chapman & Hall/CRC Press; 2002.
[31] Turrens, J. F. Mitochondrial formation of reactive oxygen species. *J. Physiol.* **552:**335–344; 2003.
[32] Edgell, C. J.; McDonald, C. C.; Graham, J. B. Permanent cell line expressing human factor VIII-related antigen established by hybridization. *Proc. Natl. Acad. Sci. USA* **80:**3734–3737; 1983.
[33] Zhao, H.; Joseph, J.; Fales, H. M.; Sokoloski, E. A.; Levine, R. L.; Vasquez-Vivar, J.; Kalyanaraman, B. Detection and characterization of the product of hydroethidine and intracellular superoxide by HPLC and limitations of fluorescence. *Proc. Natl. Acad. Sci. USA* **102:**5727–5732; 2005.
[34] Redondo-Horcajo, M.; Romero, N.; Martínez-Acedo, P.; Martínez-Ruiz, A.; Quijano, C.; Lourenço, C. F.; Movilla, N.; Enríquez, J. A.; Rodríguez-Pascual, F.; Rial, E.; Radi, R.; Vázquez, J.; Lamas, S. Cyclosporine A-induced nitration of tyrosine 34 MnSOD in endothelial cells: role of mitochondrial superoxide. *Cardiovasc. Res.* **87:**356–365; 2010.
[35] Kalyanaraman, B.; Darley-Usmar, V.; Davies, K. J.; Dennery, P. A.; Forman, H. J.; Grisham, M. B.; Mann, G. E.; Moore, K.; Roberts 2nd L. J.; Ischiropoulos, H. Measuring reactive oxygen and nitrogen species with fluorescent probes: challenges and limitations. *Free Radic. Biol. Med.* **52:**1–6; 2012.
[36] Calvani, M.; Comito, G.; Giannoni, E.; Chiarugi, P. Time-dependent stabilization of hypoxia inducible factor-1alpha by different intracellular sources of reactive oxygen species. *PLoS One* **7:**e38388; 2012.
[37] Nijtmans, L. G.; de Jong, L.; Artal Sanz, M.; Coates, P. J.; Berden, J. A.; Back, J. W.; Muijsers, A. O.; van der Spek, H.; Grivell, L. A. Prohibitins act as a membrane-bound chaperone for the stabilization of mitochondrial proteins. *EMBO J.* **19:**2444–2451; 2000.
[38] Perry, S. W.; Norman, J. P.; Barbieri, J.; Brown, E. B.; Gelbard, H. A. Mitochondrial membrane potential probes and the proton gradient: a practical usage guide. *Biotechniques* **50:**98–115; 2011.
[39] Becker, L. B.; vanden Hoek, T. L.; Shao, Z. H.; Li, C. Q.; Schumacker, P. T. Generation of superoxide in cardiomyocytes during ischemia before reperfusion. *Am. J. Physiol.* **277:**H2240–H2246; 1999.

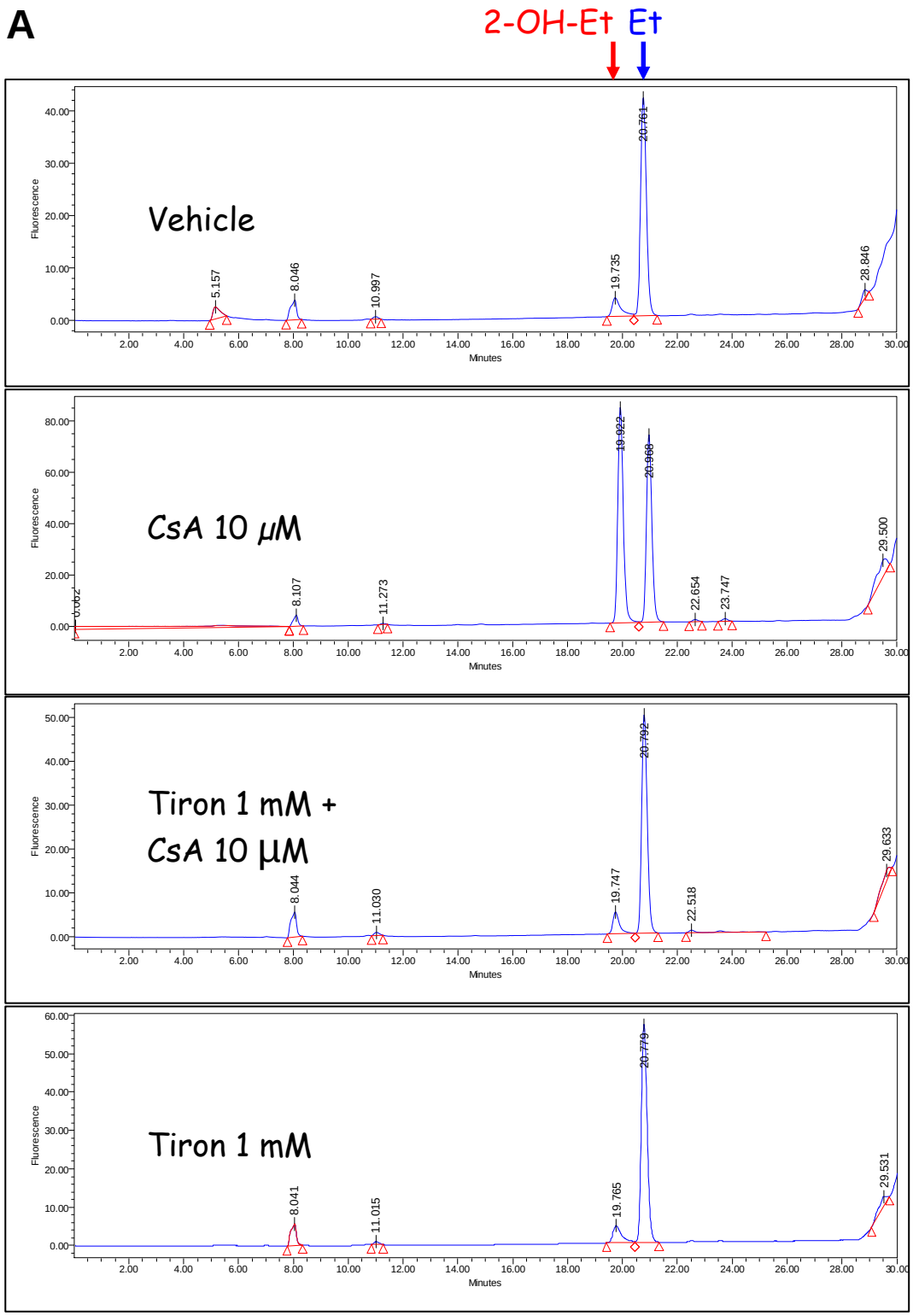

Supplementary Figure 1. **A.** Chromatograms from control experiments showing the separation of the peaks corresponding to 2-hyroxyethidium (2-OH-Et, the specific product of superoxide reaction with DHE) and ethidium (Et). Treatment of BAECs with cyclosporin A (CsA) induced superoxide anion production (Redondo-Horcajo *et al*., ref. [34]), which was abolished by treatment with 1 mM Tiron.

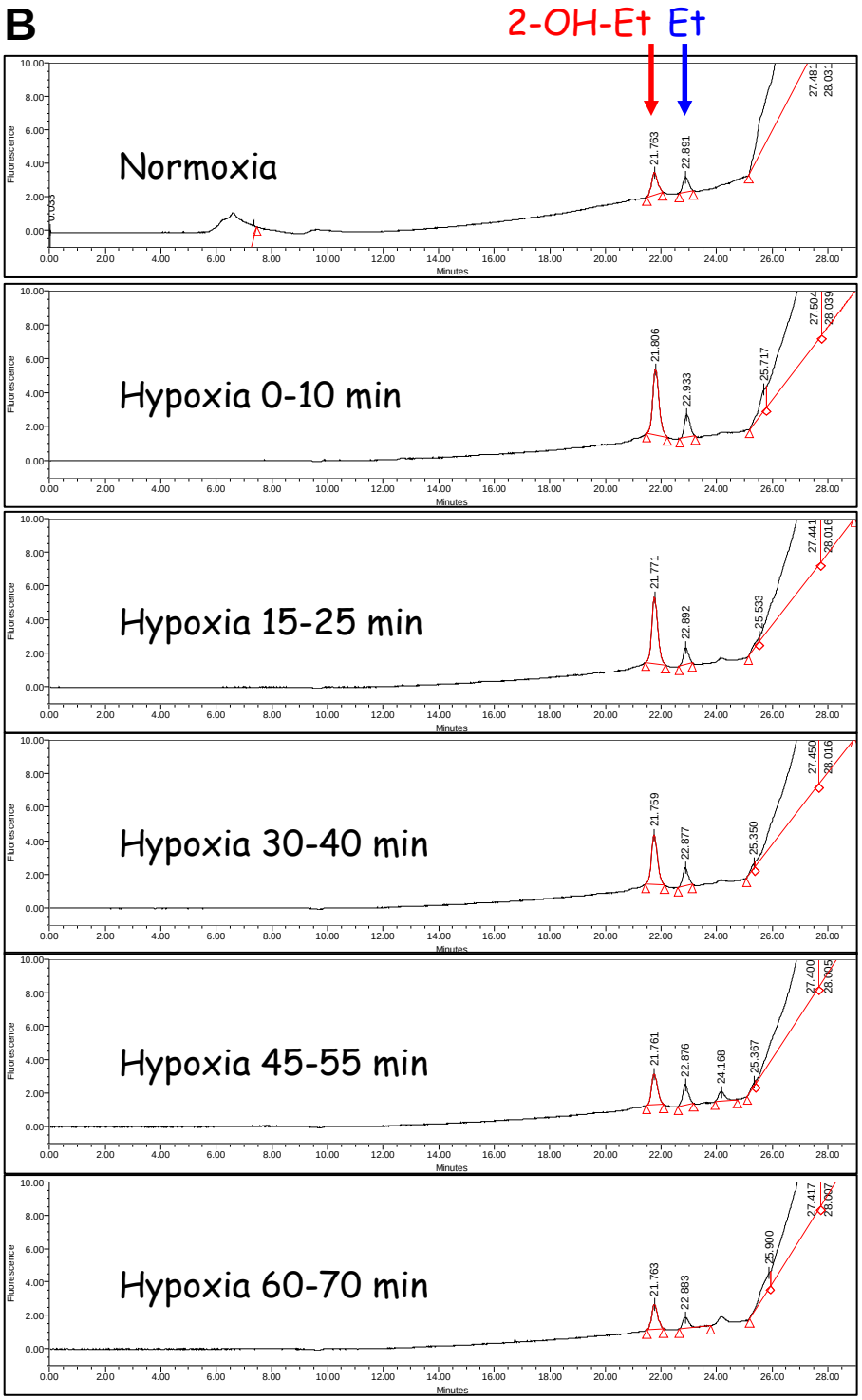

Supplementary Figure 1. B. Chromatograms from a representative experiment included in Figure 2. Exposure of BAECs to hypoxia increased the area of 2-OH-Et peak in the first minutes, decreasing to normoxic values thereafter (quantified in Figure 2), independently of the Et peak.

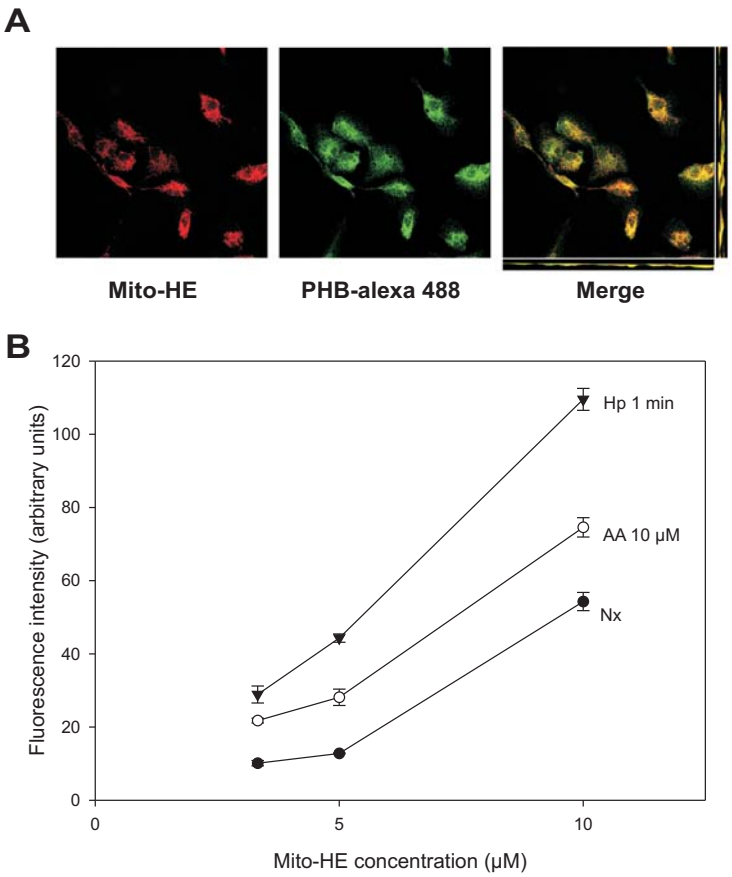

Supplementary Figure 2

(A) Colocalization of Mito-HE and the mitochondrial marker prohibitin in fixed endothelial cells BAEC were incubated with 5 μM Mito-HE for 10 min, fixed and immunostained with anti-prohibitin (PHB) antibody. Representative images show mitochondrial localization of Mito-HE.

(B) Mitochondrial superoxide detection by Mito-HE at different concentrations. BAECs were treated as in Figure 1, but incubated with different Mito-HE concentrations. Quantification of images from three independent experiments. The concentration used in the rest of experiments is 5 μM Mito-HE.

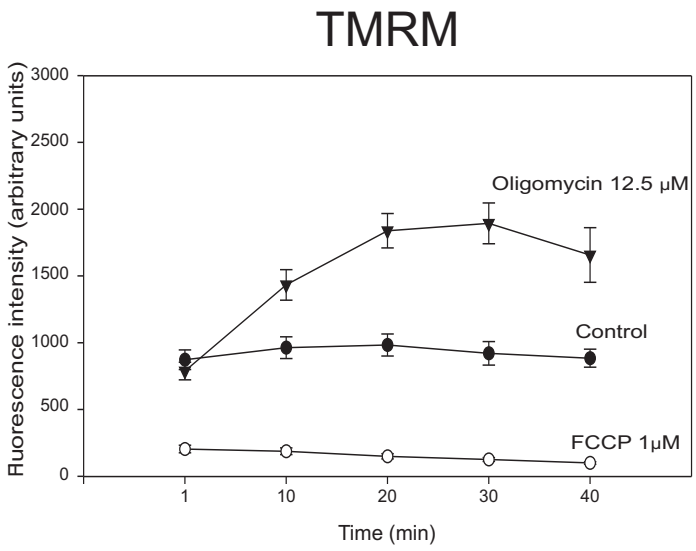

Supplementary Figure 3

Mitochondrial membrane potential measurement by fluorescence microscopy in live untreated endothelial cells and treated with oligomycin or FCCP. BAECs were treated as in Figure 8D, but with addition of oligomycin or FCCP prior to normoxic or hypoxic (2% O_2) incubation Quantification of four regions for three independent experiments is plotted for each time as mean s.e.m. Black circles: control; white circles: FCCP treatment; black inverted triangles: oligomycin treatment.

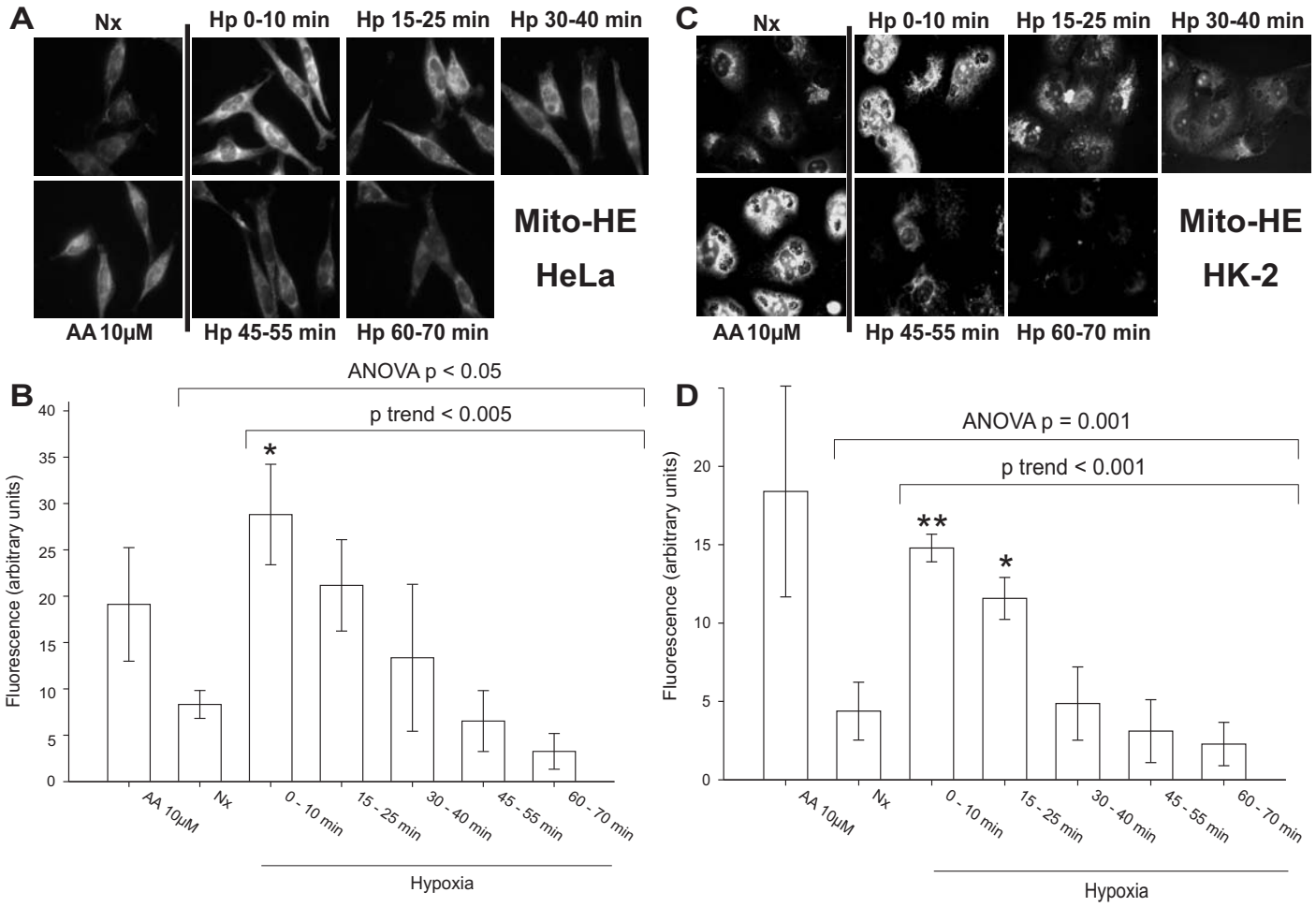

Supplementary Figure 4

Mitochondrial superoxide detection by Mito-HE and fluorescence microscopy in fixed tumor cells. HeLa **(A, B)** and HK2 cells **(C, D)** were treated as in Figure 1. 5 μM Mito-HE was added for 10 min more, and cells were fixed in the hypoxia chamber. **(A, C)** Representative images showing Mito-HE fluorescence. **(B, D)** Quantification of images from three independent experiments. Data are presented as mean s.e.m. * $p < 0.05$, ** $p < 0.01$ versus Nx.

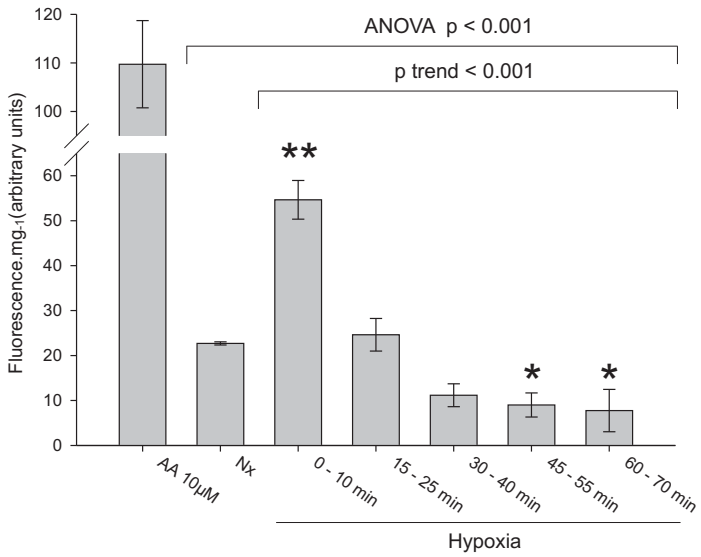

Supplementary Figure 5

Superoxide detection by DHE and HPLC in HeLa. HeLa cells were treated as in Figure 1. After DHE incubation (5 µM DHE, 10 min) cells were lysed in the hypoxia chamber, frozen and 2-OH-E amount was analyzed by HPLC with fluorescent detection. Data are presented as mean s.e.m. of three independent experiments. ** $p < 0.01$ versus Nx, * $p < 0.05$ versus Nx.

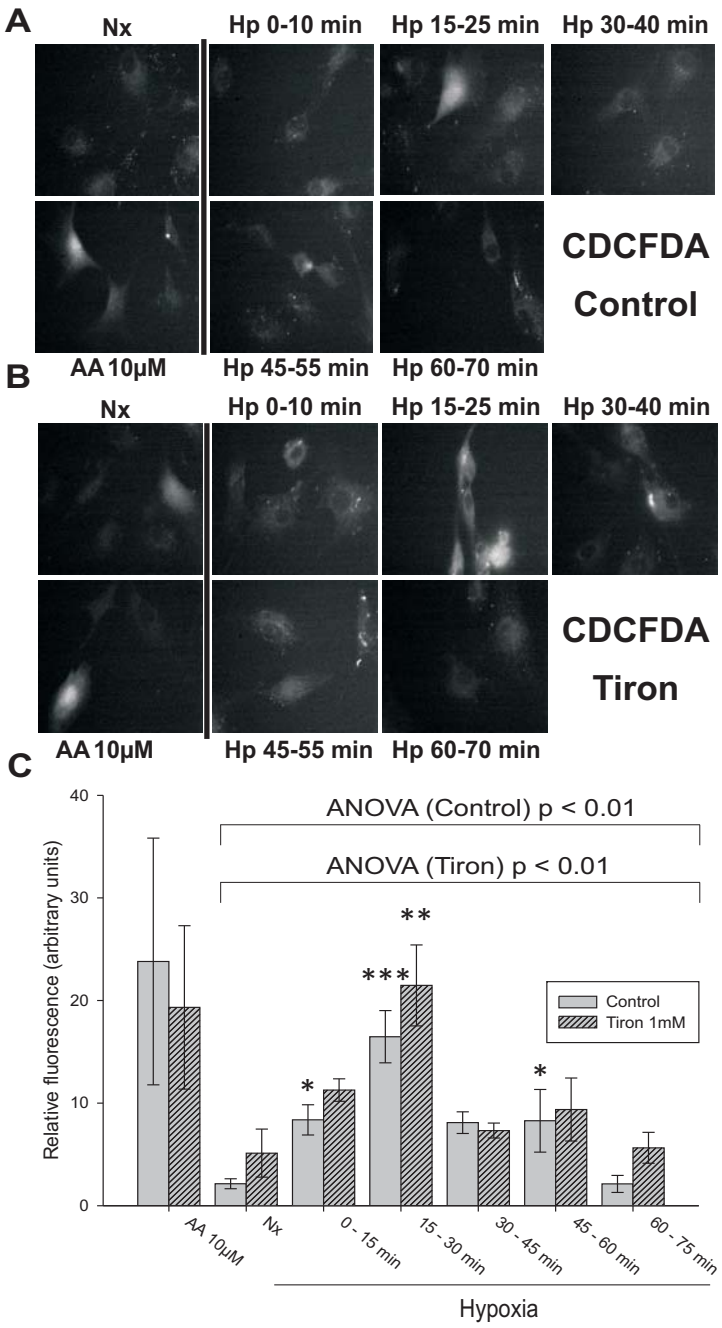

Supplementary Figure 6

ROS detection by CDCFDA and fluorescence microscopy in fixed endothelial cells treated with 1 mM Tiron. Control BAECs **(A)** and BAECs incubated with 1 mM Tiron **(B)** were treated as in Figure 1. 10 μM CDCFDA was added for 15 min more, and cells were fixed in the hypoxia chamber. **(A, B)** Representative images showing CDCFDA fluorescence. **(C)** Quantification of images from three independent experiments. Data are presented as mean s.e.m. *** $p < 0.001$ versus Nx, ** $p < 0.01$ versus Nx, * $p < 0.05$ versus Nx of each condition.